The glacial North Atlantic Oscillation

Flávio Justino and W. Richard Peltier

Department of Physics, University of Toronto

Flávio Justino and W. Richard Peltier

60 St. George Street,

Toronto, Ont. M5S 1A7 Canada

(fjustino@atmosp.physics.utoronto.ca)

Abstract

Based upon coupled climate simulations driven by present day and glacial boundary conditions we demonstrate that the glacial North Atlantic Oscillation was characterized by four distinct centres of action and thus by an atmospheric circulation that differed radically in terms of its internal variability from modern conditions. Moreover, we show that although simulated modern climate supports a coupled atmosphere-ocean mode characterized by a timescale near 30 years, this mode is predicted to be absent under LGM conditions.

1. Introduction

It has long been recognized that the North Atlantic Oscillation (NAO) exerts a strong influence upon wintertime climate over North America and Eurasia(*Rogers* [1990], *Wallace and Gutzler* [1981], *van Loon and Rogers* [1978], *Walker* [1924]), as well as on marine, terrestrial and freshwater ecosystems (*Ottersen* [2001]). Despite its importance, the issue as to how the NAO has changed in the past or will vary in the future is unknown (*Cook* [2003]). For example, it is as yet unresolved as to whether NAO derived extratropical climate variability at Last Glacial Maximum (LGM) was stronger or weaker than it is at present. During that period land characteristics were different from those observed at present, in the sense that parts of North America and northern Europe were covered by vast ice sheets (see Fig. 1b). Climate simulations (e.g. *Justino et al.* [2005], *Peltier and Solheim* [2004], *Shin et al.* [2003], *Hewitt et al.* [2001], *Vettoretti et al.* [2000], *Dong and Valdes* [1998], *Broccoli and Manabe* [1987], *Rind* [1987]) have demonstrated that mean climate state at LGM was significantly different as compared to today, which raises the possibility that a distinct form of polar climate variability may also have existed during the glacial period.

Despite extensive studies of the climate processes governing the NAO, many controversial issues remain. While it has long been recognized that the NAO owes its essential existence to atmospheric dynamical processes (*Thompson et al.* [2003]), results of global coupled model (GCM) simulations driven by present day boundary conditions suggest a modification of this view (*Rodwell et al.* [1999], *Timmermann et al.* [1998]). In particular, it has been suggested (*Rodwell et al.* [1999]) that a large fraction of the inter-annual to inter-decadal variability of the winter NAO may be reconstructed on the basis of sea surface temperature (SST) variations. Furthermore, GCM results have demonstrated that changes in the North Atlantic thermohaline circulation and associated heat flux may lead to a reversal of the phase of the NAO (*Timmermann et al.* [1998]). These issues may be further investigated in detail using GCM integrations designed to reproduce LGM climate. The presence of glacial ice sheets (Fig. 1b) exerts a strong influence upon the glacial wintertime atmospheric circulation over the North Atlantic due both to the mechanical forcing associated with the marked change in surface topography, and with the thermal forcing related to enhanced ice albedo feedback. Thus, on decadal and inter-decadal timescales the changes in air-sea fluxes and in the thermohaline circulation may result in a significantly modified spatial and temporal variability of the NAO.

2. The model and the coupled climate

The coupled atmosphere-ocean-sea-ice model employed in this study is the NCAR-CCSM (*Kiehl et al.* [1998]). The atmospheric general circulation model that we employ is the low resolution version of CCSM 1.4 that incorporates 18 vertical levels in which the model fields are truncated triangularly at degree and order 31, which corresponds to 96 by 48 longitude and latitude grid points. The dynamics of the ocean are described on 25 vertical levels on a 3 degree by 3 degree grid. Additionally, the coupled model includes a sophisticated sea-ice component as well as a simplified representation of land surface processes.

In order to investigate the *glacial NAO* two model simulations have been performed: A modern simulation driven by present day boundary conditions (MOD) and a second experiment for the LGM (*Peltier and Solheim* [2004], *Peltier and Solheim* [2002]). In order to allow intercomparison of model simulations of LGM climate, the Paleoclimate Modelling Intercomparison Project (PMIP, http://www-lsce.cea.fr/pmip) has established a protocol for setting the four major boundary conditions that are required for the purpose of such analyses as follows: (I) orbital parameters are to be fixed to those corresponding to 21000 years ago, (II) ice sheet topography and albedo are to be fixed according to the ICE-4G or ICE-5G models (*Peltier* [1994], *Peltier* [2004]), (III) the land-sea mask and paleo sea level are also to be fixed according to the ICE-4(5)G models, (IV) the concentrations of the radiatively active atmospheric trace gases (CO_2, CH_4 and N_2O) are also to be adjusted based upon estimates from the Vostok ice core.

The MOD (LGM) experiment was run to equilibrium for 2000 (2500) years (*Peltier and Solheim* [2004], *Peltier and Solheim* [2002]) and the analyses discussed herein are based upon the last 500 years of each simulation. We focus on the winter season of the Northern Hemisphere (NH) (December, January and February - DJF) when the NAO is characterized by the largest anomalies of the sea level pressure over the North Atlantic under modern climate conditions. It is important to realize that long climate integration of the kind under discussion here have never been produced previously at the relatively high spatial and temporal resolution that we have employed. Such long climate simulations are required to obtain reliable analyses of periodicities of climate features and may be expected to improve our understanding of the dynamical processes governing the principle modes of climate variability.

The annually and globally averaged SST in the MOD and LGM simulations are respectively near 18.5°C and 14.5°C (*Peltier and Solheim* [2004], *Peltier and Solheim* [2002]), implying a drop in the mean of approximately 4°C. SST anomalies in the polar and mid-latitude regions, however, may reach values as high as -9°C. Obvious by inspection of Fig. 1b is the substantial increase of the sea-ice in the NH under LGM conditions, with the southern boundary of essentially perennial sea-ice markedly shifted to lower latitude. These modifications of surface ocean conditions lead to a significant reduction in the strength of NADW production and a simultaneous reduction in the depth to which NADW penetrates. Under modern conditions, the strength of the Atlantic MOC is predicted to be approximately 20Sv ($1Sv = 10^6 m^3 s^{-1}$) and to extend to a depth of about 2km, whereas under LGM conditions it is predicted to be approximately 12 Sv and it is confined to a depth of approximately 1km (*Peltier and Solheim* [2004], *Peltier and Solheim* [2002]).

The simulated present day mean eddy sea level pressure (i.e., the sea level pressure with the zonal mean removed) corresponds closely to NCEP reanalysis data (*Kalnay et al.* [1996]) (Fig. 2a). The inclusion of the LGM boundary conditions, however, drastically changes the sea level pressure (SLP) distribution as compared to the modern simulation. Figure 2b shows that over the extratropical region an increase in the predicted glacial SLP develops that is primarily due to enhanced surface cooling and the attendant increase of atmospheric stability. Accompanying the increase in SLP in the LGM simulation there is also a predicted weakening of the Aleutian and Icelandic lows as a result of reduced latent and sensible heat fluxes from the ocean to the atmosphere. These results are in close accord with previous LGM simulations (*Kitoh et al.* [2001], *Cook and Held* [1988], *Broccoli and Manabe* [1987], *Rind* [1987]). The increase in sea-ice extent insulates the atmosphere from the underlying warmer ocean, thus cutting off the transfer of heat from the ocean to the atmosphere (see Fig. 1b).

As one might expect, the anomalous stationary atmospheric Rossby wave structure, as well as the changes in SST and sea-ice predicted by the LGM simulation, strongly modify the baroclinic and barotropic structure of the atmosphere and play a key role in determining the nature of the *glacial NAO*.

3. Temporal and spatial climate variability

In what follows we investigate the temporal and spatial structure of the NAO based on empirical orthogonal function (EOF) and spectral analysis. Based upon a standard EOF analysis, the NAO is identified from the eigenvectors of the cross-covariance matrix obtained by calculating the time variations of the grid-point values of SLP. The NAO is herein displayed in terms of its amplitude (Fig. 3a,d), obtained by regressing the hemispheric sea level pressure anomalies upon the leading principal component (PC) time series from the North Atlantic domain (20°-70°N, 90°W-40°E).

The leading pattern of variability in the MOD simulation (Fig. 3a,b) is characterized by the existence of a well known characteristic dipolar structure over the North Atlantic, which is dominated by two areas of strongest out-of-phase variability located over Iceland and the Azores/Iberian Peninsula (e.g. *Thompson et al.* [2003]). The first EOF accounts for 54% of the total variance and is well separated from the second EOF which explains

14% (not shown). When the pressure difference between the Azores and Iceland is large (small) the mid-latitude surface westerlies are strong (weak) (Fig. 3a).

In addition to the characteristic surface pressure pattern, the predicted NAO under modern climate conditions also exhibits a prominent characteristic temporal variability. This is clearly shown by the power spectrum (Fig. 3b) of the first principal component (PC) time series of SLP obtained by applying the Multi-Taper method (MTM) (*Thomson* [1982]). In order to perform the spectral analysis of the Principal Component (PC) time series, 3 tapers were employed and spectral fluctuations at frequencies greater than the Rayleigh frequency ($f_r = (N\Delta t)^{-1}$) are thereby well resolved. Here N is the length of the time series ($N = 500$) and t is the sampling interval ($t = 1year$). The frequency resolution of the spectrum is given by $2pf_r$, where p is the band width parameter ($p = 2$). This methodology allows us to resolve oscillatory signals with periods varying from interannual to interdecadal. From Figure 3b it is evident that the NAO exhibits a significant concentration of power at interannual timescales of 2-4 years and at a multidecadal timescale near 30 years period which is dominant. Some enhancement of power is also evident in the 6-8 year band, but this is significant only at the 95% level. This result agrees with previous analyses based on coupled model simulations (*Timmermann et al.* [1998], *Delworth et al.* [1993], *James and James* [1989]) as well as with results based on climate reconstructions (*Mann et al.* [1998], *Cook et al.* [1998], *Rogers* [1984]) from tree-rings and other proxies insofar as the existence of the multi-decadal signal is concerned. To provide an initial investigation of the interplay between the atmosphere and the ocean which supports the multi-decadal signal, the power spectrum for the first PC time series of SST calculated in the North Atlantic domain (20°-70°N, 90°W-40°E) has also been computed (Fig. 3c). The spectrum of the SST is almost "red" (i.e., power increasing with period) but also clearly reveals the strong concentration of power at the same timescale near 30 years. Given this we may conclude that the interannual variability of the NAO is associated with the behavior of the atmosphere alone. At longer time scales, however, it is equally clear that air-sea coupling is significantly involved (*Czaja et al.* [2003], *Feldstein* [2000], *Rodwell et al.* [1999], *Timmermann et al.* [1998]).

In order to study the *glacial NAO* identical EOF analyses were performed on the results obtained from the LGM simulation. These results reveal a markedly different picture compared to the results obtained from the modern simulation (Figs. 3d-f). Due to the presence of striking SLP anomalies in the LGM simulation (see Fig. 2b), the leading EOF for the glacial period is characterized by the existence of multiple centres of action over high latitudes. The first EOF in the LGM run explains 59% of the total variance compared to 54% in the MOD simulation. It is interesting to note, moreover, that the surface pressure field is characterized by the existence of a quadrapolar structure with distinct centres of action over North America/Labrador Sea, over Siberia, over the Mediterranean Sea/Iberian Peninsula and over the North Pacific/Aleutian Islands (Fig. 3d). This result demonstrates that the north-south dipole of SLP anomalies over the North Atlantic that is characteristic of the present day NAO is shifted into an approximately east-west alignment in the LGM simulation. According to a simple quasi-geostrophic assumption, this SLP pattern would be associated with strongly meridional wind anomalies over the North Atlantic instead the zonal nature of the anomalous wind characteristic of the NAO under modern conditions (see the arrows on Fig. 3a,d indicating the lines of strongest SLP gradient which are approximately normal to the directions of anomalous wind). Furthermore, over Eurasia a different atmospheric flow configuration is expected to be characteristic of high latitude variability as compared to modern conditions. When the EOF analysis is extended to include the SLP field for the entire polar region, rather than being restricted to the North Atlantic sector, we obtain a leading EOF that is essentially identical to that shown on Figure 3a,d (not shown). We therefore assert that the LGM form of the Arctic Oscillation also has the same quadrapolar structure as the NAO.

The leading EOF in the LGM simulation also differs from its MOD counterpart over mid-latitudes. Whereas the southern centre of action is located near the Azores in the MOD simulation, this centre is shifted eastward over the Mediterranean region in the LGM simulation (*Peltier and Solheim* [2002]). Moreover, it is important to note the appearance of larger amplitude SLP anomalies over the North Pacific and their in-phase relationship with the changes over the Mediterranean region. This demonstrates that the topographic forcing and ice albedo feedback are both crucial to generating the quadrapolar form of the atmospheric variability, primarily due to the attendant modifications of the stationary and transient waves. Indeed, it has been shown previously that the LGM atmospheric circulation was characterized by highly significant changes of both transient and stationary waves (*Justino et al.* [2005], *Peltier and Solheim* [2004], *Vettoretti et al.* [2000], *Broccoli and Manabe* [1987], *Rind* [1987]) which are clearly reflected in the temporal and spatial variability of the NAO (*Thompson et al.* [2003]).

The incorporation of LGM boundary conditions also induces a distinct temporal variability of the *glacial NAO* as compared to the MOD simulation (Fig. 3e). The power spectrum of the *glacial NAO* is almost white but reveals somewhat enhanced variance near a period of 3 years. No other peak in the spectrum is significant at the 99% level. Additionally, Figures 3b,e demonstrate that the slightly enhanced power at 4-5 year periods in the MOD simulation is somewhat weaker in the LGM run. The latter experiment does reveal, however, an intensification in the sub-decadal period range from 5-10 year. The most striking difference between the LGM and MOD spectra of SLP, however, is the absence of the 30 year cycle in the LGM run. It should also be noted that the 30 year peak is entirely absent from the spectrum defined by the first PC time series of the North Atlantic SST calculated from the glacial simulation (Fig. 3f). To provide additional evidence for the link between the atmosphere and the underlying ocean we show in Figure 4a,b the power spectrum of the strength of the Atlantic meridional overturning circulation (MOC) for both the present day and the LGM simulations. In agreement with spectral analyses of the present day SST and SLP, the spectrum of the present day MOC shows a significant peak with a period of approximately 30 years (Fig. 4a). This signal is entirely absent from the results of the spectral analysis performed for the Atlantic MOC under LGM conditions (Fig. 4b).

Computations of the lagged regression between the present day MOC index and the SLP anomalies over the North Atlantic show that, at lag 0, a weakening of the MOC is accompanied by a positive amplitude phase of the NAO. Correlation analysis also shows that these time series are anti-correlated to a high degree (with a coefficient of -0.55).

Similar calculation for the MOC and the first PC of SST shows, however, that these fields are uncorrelated. Low correlation was also found between the first PC of SST and SLP. Turning to analyses of the LGM conditions, these reveal that the strength of the Atlantic MOC and the PC1 of SST (SLP) are anti-correlated with a correlation coefficient of -0.35 (-0.45). It is interesting to note the high correlation (up to 0.6) between the leading PC of SST and SLP. In fact, this high correlation between SST and SLP is associated with the extensive sea-ice concentration that is captured in the EOF analysis of the glacial SST. This is evident by the high anti-correlation (-0.9) between the first PC of SST and the first PC of sea-ice. On the basis of these analyses it is reasonable to assume that the *glacial NAO* is not modulated by changes in the strength of the MOC, but rather is linked to the variability in sea-ice extent. This is illustrated on Figure 4d that shows the high correlation between the SLP and sea-ice variability. Variations in the area covered by sea-ice induce stationary wave anomalies due primarily to changes of the forcing of the atmosphere due to surface heating (*Justino et al.* [2005], *Peltier and Solheim* [2004], *Vettoretti et al.* [2000], *Broccoli and Manabe* [1987]). In addition, variations in sea-ice area cause significant changes in the rate of deep water formation and consequently in the amount of heat transported northward (*Czaja et al.* [2003], *Speer and Tziperman* [1992]).

4. Summary and concluding remarks

Based on coupled climate simulations performed under present day and glacial boundary conditions, our analyses provide evidence that under modern climate conditions there exists a coupled climate mode characterized by a timescale of approximately 30 years. This mode has been clearly identified in spectral analysis performed on both atmospheric and oceanic variables. It appears to be closely associated with anomalous oceanic surface conditions. This marked feature of the modeled present day climate is completely absent in our simulation of LGM climate. The NCAR-CCSM model predicts substantial changes in the form and the temporal variability of the *glacial NAO* as compared to the modern NAO. These changes are clearly caused by the presence of the Laurentide and Scandinavian ice sheets which induce profound changes of the stationary waves, sea-ice extent and the oceanic meridional overturning circulation. The extended region that is predicted to have been covered by perennial sea-ice in the North Atlantic increases oceanic stability and reduces air-sea coupling thus affecting the wind-driven circulation. A substantial weakening of the temporal variability of North Atlantic Deep Water (NADW) production may therefore be expected and we have found this to be the case. The *glacial NAO* is characterized by four centres of action located over North America/Labrador Sea, over Siberia, over the Mediterranean Sea/Iberian Peninsula and over the North Pacific. While during the positive phase of the modern NAO a strong westerly flow develops over the Atlantic Ocean, in the *glacial NAO* an enhanced southerly wind develops over this region, whereas cyclonic winds dominate the atmospheric flow over Siberia. These changes in the structure of extra-tropical climate variability will have to be carefully considered when temperature or precipitation/snowfall are estimated from paleo-proxy data for the Last Glacial Maximum interval.

5. Acknowledgments

We are grateful to Dr. Guido Vettoretti for his assistance in the initial analyses of the model output data.

References

Broccoli, A., and S. Manabe (1987), The influence of continental ice, atmospheric CO_2 and land albedo on the climate of the last glacial maximum , *Clim. Dyn.*, *1*, 87–99.

Cook, E. (2003), Multi-Proxy Reconstructions of the North Atlantic Oscillation (NAO) Index: A Critical Review and a New Well-Verified Winter NAO Index Reconstruction Back to AD 1400, in *The North Atlantic Oscillation*, pp. 63–79, AGU, Geophysical Monograph Series.

Cook, E., R. D. D'arrigo, and K. R. Briffa (1998), A reconstruction of the North Atlantic Oscillation using tree-ring chronologies from North America and Europe, *The Holocene*, *8*, 8–17.

Cook, K., and I. Held (1988), Stationary waves of the ice age climate, *J. Clim.*, *1*, 807–819.

Czaja, A., A. Robertson, and T. Huch (2003), The role of coupled processes in producing NAO variability. An overview of the North Atlantic Oscillation, in *The North Atlantic Oscillation*, pp. 147–172, AGU, Geophysical Monograph Series.

Delworth, T. L., S. Manabe, and R. Stouffer (1993), Interdecadal variations of the thermohaline circulation in a coupled ocean-atmosphere model, *J. Clim.*, *6*, 1993–2011.

Dong, B., and P. Valdes (1998), Simulation of the last glacial maximum climates using a general circulation model: Prescribed versus computed sea surface temperature., *Clim. Dyn.*, *14*, 571–591.

Feldstein, S. B. (2000), Teleconnections and ENSO: The timescale, power spectra, and climate noise properties, *J. Clim.*, *13*, 4430–4440.

Hewitt, C. D., A. Broccoli, J. Mitchell, and R. J. Stouffer (2001), A coupled model of the last glacial maximum: was part of the North Atlantic relatively warm?, *Geophys. Res. Lett.*, *28*, 1571–1574.

James, I. N., and P. M. James (1989), Ultra-low-frequency variability in a simple atmospheric circulation model. nature, 342, 53-55, *Nature*, *342*, 53–55.

Justino, F., A. Timmermann, U. Merkel, and E. Souza (2005), Synoptic reorganisation of atmospheric flow during the Last Glacial Maximum, *J. Clim.*, in press.

Kalnay, E., et al. (1996), The NCEP-NCAR 40 Year Reanalysis Project, *Bull. Amer. Soc.*, *77*, 437–471.

Kiehl, J. T., J. Hack, G. Bonan, B. Boville, D. Williamson, and P. Rasch (1998), The National Center for Atmospheric Research Community Climate Model: CCM3 , *J. Clim.*, *11*, 1131–1149.

Kitoh, A., S. Mukarami, and H. Koide (2001), A simulation of the Last Glacial Maximum with a coupled atmosphere-ocean GCM, *Geophys. Res. Lett.*, *28*, 2221–2224.

Mann, M., J. Park, and R. S. Bradley (1998), Global interdecadal and century-scale oscillations during the past five centuries, *Nature*, *378*, 266–270.

Ottersen, G. (2001), Ecological effects of the North Atlantic Oscillation, *Oecologia*, *128*, 1–14.

Peltier, W. (1994), Ice age paleotopography, *Science*, *265*, 195–201.

Peltier, W. (2004), Global glacial isostasy and the surface of the ice-age Earth: the ICE-5G (VM2) model and GRACE, *Annual Review of Earth and Planetary Sciences.*, *32*, 111–149.

Peltier, W., and L. Solheim (2004), The climate of the Earth at Last Glacial Maximum: statistical equilibrium state and a mode of internal variability, *Quaternary Science Reviews*, (23), 335–357.

Peltier, W. R., and L. P. Solheim (2002), Dynamics of the ice age Earth: Solid mechanics and fluid mechanics, *J. Phys. IV*, *12*, 85–104.

Rind, D. (1987), Components of the ice age circulation, *J. Geophys. Res*, *92*, 4241–4281.

Rodwell, M. J., D. P. Rowell, and F. K. Folland (1999), Oceanic forcing of the wintertime North Atlantic Oscillation and European climate , *Nature*, *398*, 320–323.

Rogers, J. C. (1984), The association between the North Atlantic Oscillation and the Southern Oscillation in the North Hemisphere, *Mon. Wea. Rev.*, *112*, 1999–2015.

Rogers, J. C. (1990), Patterns of low-frequency monthly sea-level pressure variability (1899 - 1986) and associated wave cyclone frequencies, *J. Clim.*, *3*, 1364–1379.

Shin, S. I., Z. Liu, B. L. O. Bliesner, E. B. amd J.E. Kutzbach, and S. P. Harrison (2003), A simulation of the Last Glacial Maximum Climate using the NCAR CSM, *Clim. Dyn*, *20*, 127–151.

Speer, K., and E. Tziperman (1992), Rates of water mass formation in the North Atlantic Ocean, *J. Phys. Oceanogr.*, *22*, 94–104.

Thompson, D. W., S. Lee, and M. P. Baldwin (2003), Atmospheric Process Governing the Northern Hemisphere Annular Mode/North Atlantic Oscillation, in *The North Atlantic Oscillation*, pp. 81–112, AGU, Geophysical Monograph Series.

Thomson, D. J. (1982), Spectrum estimation and harmonic analysis, *Proc. IEEE*, *70*(9), 1055–1094.

Timmermann, A., M. Latif, R. Voss, and A. M. Grötzer (1998), Northern Hemisphere Interdecadal Variability: A Coupled Air-Sea Mode, *J. Clim.*, *11*, 1906–1930.

van Loon, H., and J. C. Rogers (1978), The seesaw in winter temperatures between Greenland and Northern Europe. Part I: general description, *Mon. Weather Rev*, *106*, 296–310.

Vettoretti, G., W. R. Peltier, and N. A. McFarlane (2000), Global water balance and atmospheric water vapour transport at Last Glacial Maximum: Climate simulations with the CCCma atmospheric general circulation model, *Canadian Journal of Earth Sciences*, *37*, 695–723.

Walker, G. T. (1924), Correlations in seasonal variations of weather , *Tech. Rep. 25*, IX Mem. Indian Meteorol. Dept., 275-332.

Wallace, J. M., and D. Gutzler (1981), Teleconnections in the geopotential height field during the Northern Hemisphere winter, *Mon. Wea. Rev.*, *109*, 784–812.

Figure Legends

Figure 1. Northern Hemisphere planetary topographic height [m], SST [°C] and ice cover. Values smaller than 30 pertain to SST and larger than 30 to topographic height. The panel (a) depicts present day conditions and the panel (b) LGM conditions. Ice on the surface of the continents is specified according to the ICE-4G model (*Peltier* [1994]). The oceans are colored according to the DJF mean SST obtained from the MOD and LGM simulation respectively.

Figure 2. Distribution of eddy mean sea level pressure [hPa] in DJF for MOD simulation (a) and (b) the respective anomalies between the LGM and MOD simulations.

Figure 3. Leading EOF of the winter sea level pressure (SLP) anomalies in the North Atlantic sector (20°-90°N, 90°W-40°E) for the modern simulation (a) and the LGM counterpart (d). The patterns are displayed as amplitudes (hPa) by regressing hemispheric SLP anomalies upon the standardized first principal component time series. PI, PA, PS and PP are the main centres of action over Iceland, Azores, Siberia and the North Pacific, respectively. (b) and (e) are the MTM power spectrum for the first PC of SLP in the MOD and LGM simulations. (c) and (f) are the same as in (b) and (d) but calculated for SST. Also shown is the corresponding confidence levels (smooth lines), 90%, 95% and 99% for significance relative to the null hypothesis (red noise).

Figure 4. MTM power spectrum of the time evolution of the NADW. (a) MOD simulation and (b) LGM simulation. (c), (d) shows the calculated lag correlation coefficient between the first PC of SLP and the correspond PC of sea-ice concentration for MOD and LGM simulations.

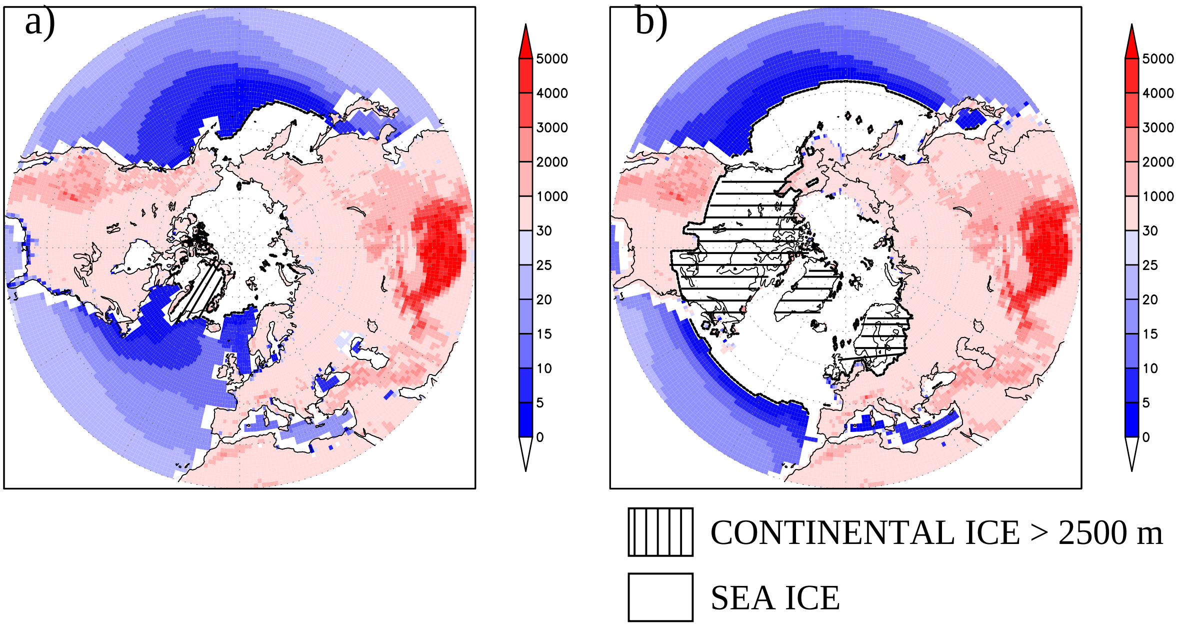
a)
b)
5000
4000
3000
2000
1000
30
25
20
15
10
5
0
CONTINENTAL ICE > 2500 m
SEA ICE

Figure 1.

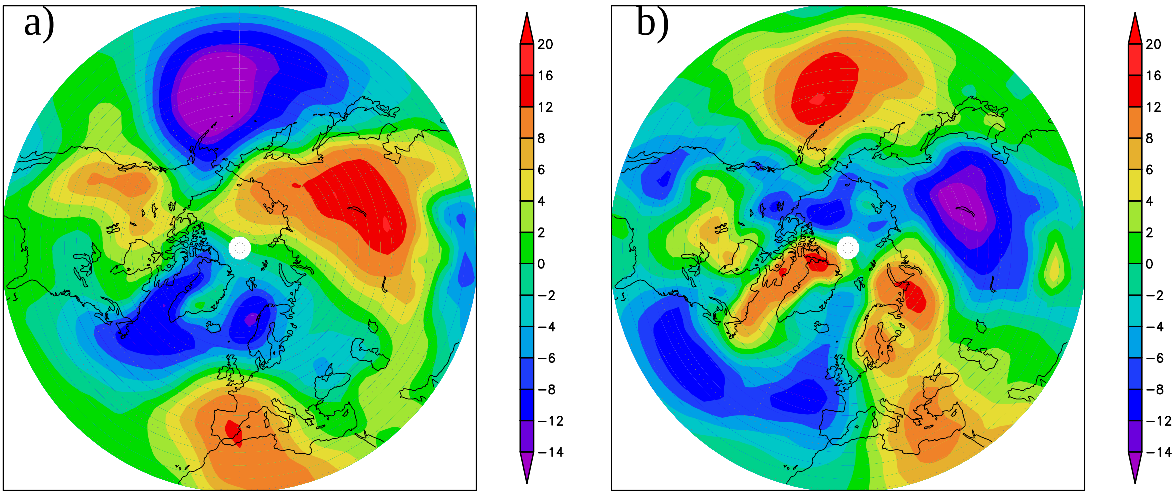

Figure 2.

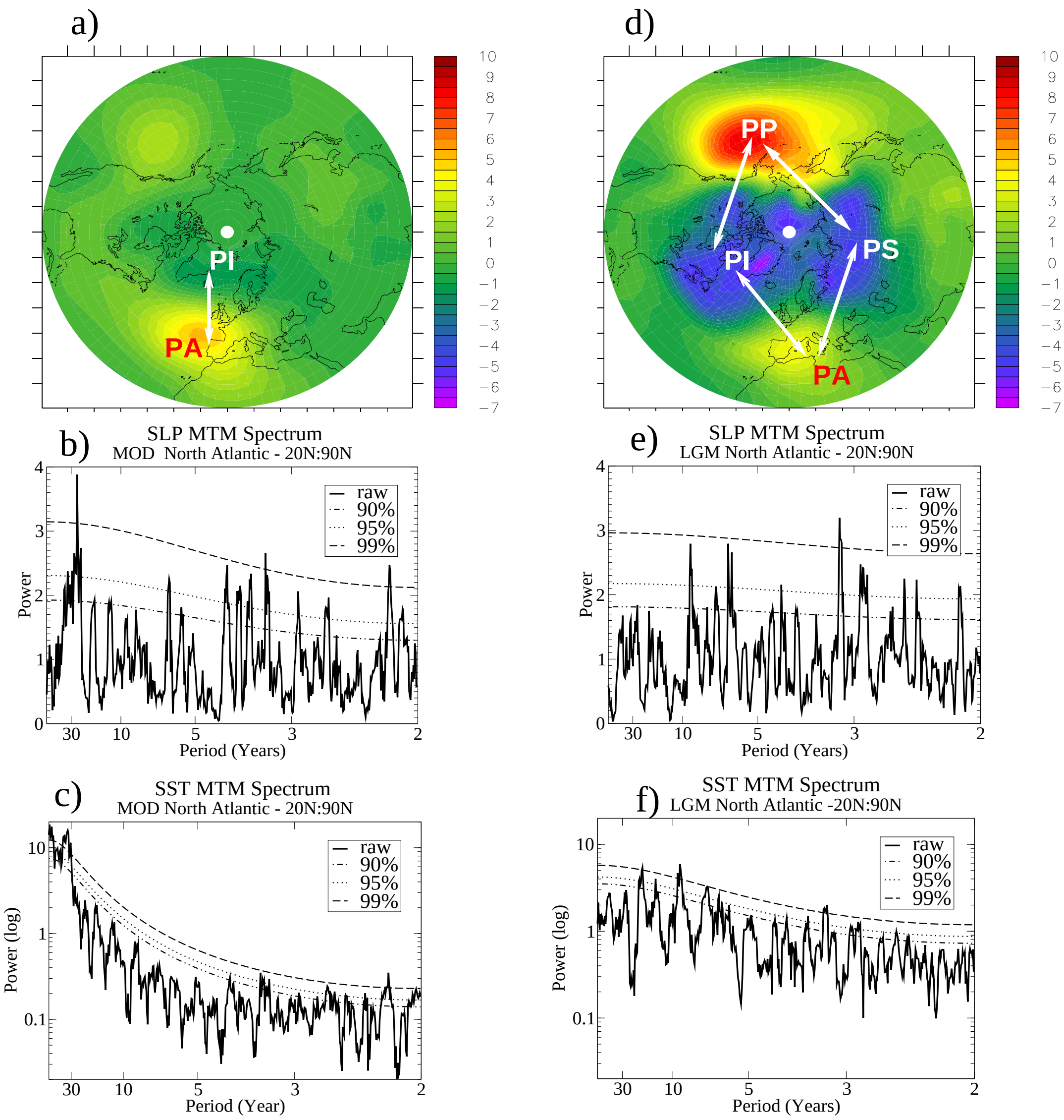

a)
PI
PA
d)
PP
PI
PS
PA
10
9
8
7
6
5
4
3
2
1
0
−1
−2
−3
−4
−5
−6
−7
b)
SLP MTM Spectrum
MOD North Atlantic - 20N:90N
e)
SLP MTM Spectrum
LGM North Atlantic - 20N:90N
Power
Period (Years)
raw
90%
95%
99%
c)
SST MTM Spectrum
MOD North Atlantic - 20N:90N
Power (log)
Period (Year)
f)
SST MTM Spectrum
LGM North Atlantic -20N:90N
Period (Years)

Figure 3.

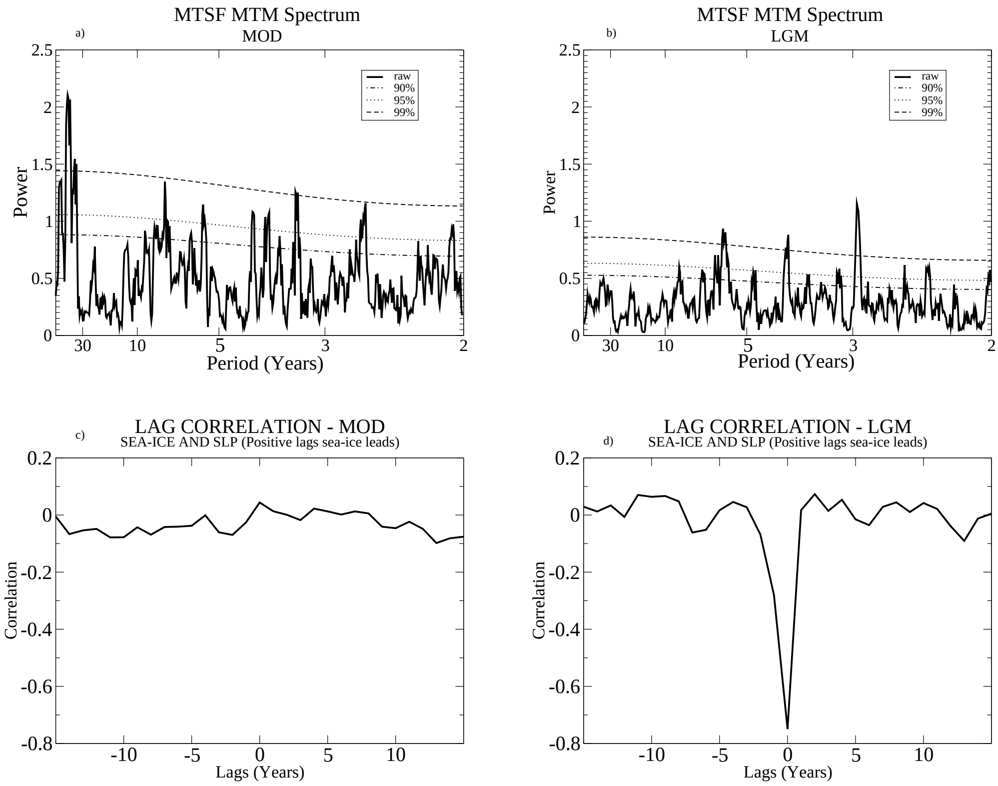
MTSF MTM Spectrum
a)
MOD
raw
90%
95%
99%
Power
Period (Years)
MTSF MTM Spectrum
b)
LGM
Power
Period (Years)
LAG CORRELATION - MOD
c)
SEA-ICE AND SLP (Positive lags sea-ice leads)
Correlation
Lags (Years)
LAG CORRELATION - LGM
d)
SEA-ICE AND SLP (Positive lags sea-ice leads)
Correlation
Lags (Years)

Figure 4.